Res Chem Intermed
https://doi.org/10.1007/s11164-018-3295-2

Novel catalytic application of Ni@ZnO nanoparticles and ZnO nanoflakes in aqueous solution of NaPTS hydrotrope at room temperature via a green synthesis of 3,4-dihydropyrimidin-2(1H)-ones

Bipin Shinde[1] · Santosh Kamble[1] · Pramod Gaikwad[1] · Vishvanath Ghanwat[1] · Sagar Tanpure[1] · Pavan Pagare[1] · Bhausaheb Karale[3] · Arvind Burungale[1,2]

Received: 19 October 2017 / Accepted: 17 January 2018

Abstract We investigated a novel catalytic application of nickel-doped zinc oxide (Ni-ZnO) nanoparticles and zinc oxide (ZnO) nanoflakes at room temperature in an aqueous hydrotropic solution for the synthesis of biologically active dihydropyrimidones (DHPMs). Ni-ZnO is a stable, recyclable, green, efficient heterogeneous catalyst which shows maximum yield in a shorter reaction time than ZnO nanoflakes in very mild conditions of hydrotropic aqueous medium for DHPMs syntheses.

Keywords Ni-ZnO · ZnO · DHPMs · Band gap · NaPTS

Introduction

Catalysis is a promising field of chemistry. There are two types of catalysis: homogeneous and heterogeneous [1]. The main advantage of homogeneous catalysis is that it gives high activities, high regio, and chemoselectivity. The main disadvantage is the recovery of the catalyst. To overcome this difficulty, heterogeneous catalysis

Electronic supplementary material The online version of this article (https://doi.org/10.1007/s11164-018-3295-2) contains supplementary material, which is available to authorized users.

✉ Bipin Shinde
bipinshinde448@gmail.com

✉ Arvind Burungale
asburungale@gmail.com

[1] Department of Chemistry, Yashavantrao Chavan Institute of Science, Satara, Maharashtra 415001, India

[2] Department of Chemistry, S.M. Joshi College, Hadpsar, Pune, Maharashtra 411028, India

[3] Department of Chemistry, Radhabai Kale Mahila Mahavidyalaya, Ahmednager, Maharashtra 414001, India

Published online: 30 January 2018

is a more suitable methodology for organic transformation. It shows excellent accessibility and stability [2], but it has some shortcomings, such as inferior catalytic performance due to reduced contact between the substrate and the catalyst. It also shows longer reaction times [3]. Therefore, new catalytic systems like nanocatalysts have been introduced to overcome the drawbacks of homogeneous catalysis. Nanomaterials act as a heterogeneous catalyst which is recovered easily and is as active as a homogeneous catalyst [4].

The reaction between urea, ethyl acetoacetate and benzaldehyde was discovered in 1893. This condensation reaction is called a Biginelli cyclocondensation reaction. The result of this Biginelli reaction is a heterocyclic system of dihydropyrimidinones (DHPMs), a multicomponent reaction in a single flask [5]. At the beginning of DHPM synthesis by Biginelli condensation, the product yield was only 25–45% [6]. The dihydropyrimidinone nucleus has received much more attention due to its active medicinal properties, for example, as antihypertensive agents, calcium channel blockers, neuropeptide Y antagonists and alpha 1a-antagonists [7–9]. Batzelladine alkaloids are the most important examples of a potent HIV group-120-CD4 inhibitor [10, 11]. DHPMs have recently received charismatic assessment due to their wide range of pharmacological and therapeutic properties, such as antibacterial, antiviral, anti-inflammatory and antitumor [12].

Recently, several methods like microwave-assisted, mechanical grinding, ultrasound reactions, etc. have been reported for the synthesis of DHPMs. These reactions are catalyzed using protic acids, Lewis acids, Bronsted acid, heteropoly acids, polyphosphate ester, clay zeolite, ferric chloride/tetraethyl orthosilicate, iodine–alumina, trimethylchlorosilane, silica gel supported-sodium hydrogen sulfate, Ziegler–Natta catalyst, sulfated tungstate, methanesulfonic acid, Nafion-H, montmorillonite K10, amberlyst-15, conc. HCl, Baker's yeast, $AlCl_3$, $[Al(H_2O)_6](BF_4)_3$, $ZnCl_2$, $CuCl_2{\cdot}2H_2O$, $FeCl_3{\cdot}6H_2O$, $LaCl_3{\cdot}7H_2O$, $LiClO_4$ [13–32], etc. These methods have limitations like a requirement for expensive reagents, highly acidic conditions, special apparatus, stoichiometric amounts of the catalyst, unsatisfactory yield, comparatively high temperature and incompatibility with other functional groups [33–35]. Most of the DHPM reactions have been carried out in solvents such as methyl cyanide, ethanol, acetonitrile, chloroform, etc., but very few reactions have been performed in water medium at room temperature. These reactions are also carried out at elevated temperatures due to a solubility problem of the multicomponent reactants in water. DHPM synthesis can also be catalyzed by using ionic liquid-like $[bmim]BF_4$ and $[bmim]PF_6$ under solvent-free conditions [36]. Especially, imidazolium-based ionic liquids contain PF_6 and BF_4 anions which are toxic in nature and liberate lethal HF; hence, the use of ionic liquids is a not much greener approach during organic transformation. Syntheses of DHPMs have also been catalyzed using PEG at an elevated temperature, 100 °C [37]. Microwave-assisted solvent-free synthesis has also been reported, but it produces internal heating by direct coupling of microwave irradiation energy with the reactants. This indicates that the proposed condensation reaction is not successful at room temperature. To overcome these limitations, we have chosen to use the sodium *p*-toluene sulfonate (NaPTS) hydrotrope which dissolves reactants in water at room temperature and can be catalyzed using Ni-ZnO nanoparticles and ZnO nanoflakes.

In recent years, hydrotropes, which are salts of low molecular weight organic compounds, have attracted extensive research interest as they have favorable properties such as high thermal stability, negligible vapor pressure and non-inflammability [38]. Hydrotropes are also known as 'green agents' due to their unique property of dissolving various organic reactants in water [39]. Hydrotropes are emerging as green agents in organic transformations. We have chosen the NaPTS hydrotrope for a proposed reaction along with distilled water because NaPTS reduces the surface tension of water. Organic solutes and water show excellent interaction in the presence of NaPTS and also show greater solubility of an organic solute in water [40]. Over the past few decades, nanocatalyzed reactions have also gained wide recognition because they can increase yield by decreasing the number of steps involved in conducting reactions and also reduce the use of chemicals and solvents [41]. Recently, the use of nanomaterials has attracted much research attention in the synthesis of heterocycles because they can positively increase the rate of reaction [42]. The Biginelli reaction is carried out in acidic conditions, and is a homogeneous acid-catalyzed reaction. Howvever, it is very tedious to remove homogeneous catalysts from the reaction mixture. The synthesis of 3,4-dihydropyrimidin-2(1H)-ones was carried in the presence of solvents like 1,4-dioxane, THF, DMF, toluene, etc.

Here, we report a catalytic application of zinc oxide nanoflakes and nickel-doped zinc oxide nanoparticles in water for the synthesis of DHPMs at room temperature. This is a novel, powerful, economical, highly efficient and extremely rapid methodology in water for the synthesis of DHPMs at room temperature. To the best of our knowledge, this is the first report of the catalytic application of ZnO nanoflakes and Ni-ZnO nanoparticles for the synthesis of DHPMs in water at room temperature in the presence of hydrotropes.

Experimental

Preparation of ZnO nanoflakes and Ni-ZnO nanoparticles

All chemicals required for the synthesis of ZnO nanoflakes and Ni-ZnO nanoparticles were analytical reagent grade such as $ZnCl_2$, NaOH, $NiCl_2$ and 2-propanol and distilled water.

A high degree of saturation was required to obtain a nucleation rate greater than the growth rate. $ZnCl_2$ (5.5 g) was dissolved in a beaker containing 200 mL distilled water at 100 °C. The whole assembly was kept in an oil bath to achieve a 100 °C temperature, and was gently stirred for 15 min. Next, 20 mL of 5 M NaOH aqueous solution was added dropwise to the $ZnCl_2$ solution. A sedimentation technique was used to separate out the precipitate. The supernatant solution was discarded and distilled water was used to wash the precipitate, and about 800 mL of distilled water was used to completely remove the NaCl, and an $AgNO_3$ solution was used to check its removal. The purified particles were then peptized with 2-propanol in the ultrasonic bath for 15 min at room temperature. Centrifugation was used to collect the particles at 4500 rpm for 20 min. Thermal treatment was given to the collected particles at 300 °C for 4 h which led to the formation of ZnO nanoflakes.

$NiCl_2$ (0.4 g) and $ZnCl_2$ (4.5 g) were dissolved in a beaker containing 200 mL distilled water at 100 °C and the solution was held in an oil bath in order to attain a 100 °C temperature. The solution of $ZnCl_2$ and $NiCl_2$ was gradually stirred for 15 min, and then 20 mL of 5 M NaOH aqueous solution was added dropwise. The supernatant solution was discarded by using a sedimentation technique so that a precipitate settled at the bottom of the beaker. Distilled water (about 100 mL) was again added to the precipitate, and the solution was filtered through Whatmann paper No. 41. Then, about 800 mL of distilled water was used to completely remove the NaCl from the precipitate and the removal was tested by using $AgNO_3$ solution. The precipitate was further peptized in a 500 mL beaker containing 100 mL of 2-propanol. The 2-propanol was removed from the precipitate by using centrifugation at 4500 rpm for 20 min. The purified particles were dried initially and then kept in a crucible for thermal treatment at 300 °C for 4 h which led to the formation of Ni doped ZnO nanoparticles.

Procedure for the synthesis of DHPMs

A one-pot condensation of ethyl acetoacetate (1 mmol), aldehyde (1 mmol), and urea (1 mmol) was carried out by using a hydrotropic solution of NaPTS in a 100 mL round-bottom flask containing 10 mL distilled water under normal temperature and pressure conditions. Ni-ZnO nanoparticles or ZnO nanoflakes (1 mol%) were, respectively, used as a catalyst. The reaction mixture was stirred by using a magnetic stirrer under normal temperature and pressure conditions. The reaction was monitored by using the TLC technique (ethyl acetate:hexane 2:8, v/v). Ethyl acetate (15 mL) was added to the reaction mixture after completion of the reaction. Finally, the reaction mixture was centrifuged at 4000 rpm for 10 min. The catalyst settled at the bottom of the reaction mixture and the product was taken out of the pot. The catalyst was washed with deionized water and ethyl acetate and then dried in an oven at 120 °C before recycling. The procedure for the synthesis of DHPMs is shown in Fig. 1.

Characterizations

The crystal structures of the ZnO and Ni-ZnO materials were characterized by using the X-ray diffraction (XRD) technique with the model Bruker D8 Advance with Cu Kα radiation ($\lambda = 1.54$ Å) in the range 2θ 20°–80°. The surface morphology and chemical composition were studied by using scanning electron microscopy (SEM) with energy dispersive X-ray spectroscopy (EDAX) using the model JEOL JSM-6360 with an operating bias voltage of 20 kV. A UV–Visible spectrophotometer, SYSTRONICS 119, was used for optical absorption study. The products were confirmed by IR, ^{1}H-NMR and ^{13}C-NMR with model lambda (Bruker) with an operating frequency of 400 Hz.

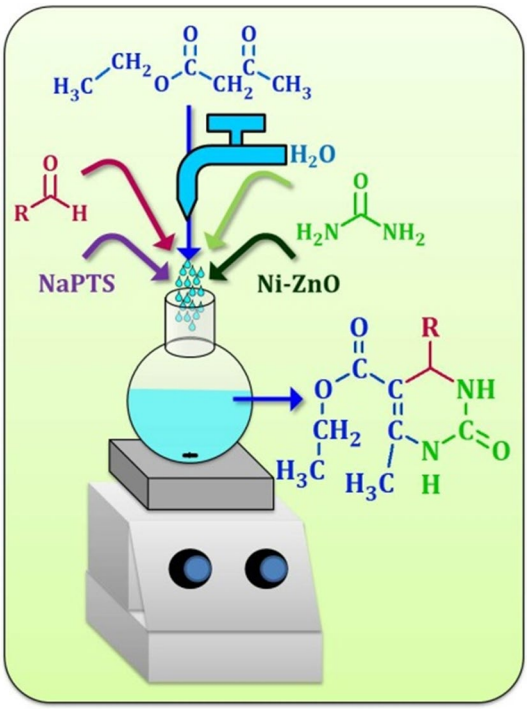

Fig. 1 Graphical representation of proposed reaction

Results and discussion

In the present study, our aim is to demonstrate the catalytic application of nanomaterials in water at room temperature for organic transformation. We decided to prepare Ni-ZnO, ZnO heterogeneous catalysts via a co-precipitation method and studied their catalytic application for the synthesis of 3,4-dihydropyrimidin-2(1H)-ones in aqueous hydrotropic solution at room temperature. Characterization of Ni-ZnO and ZnO catalysts are described below

Catalyst characterization

Optical measurement

UV–visible spectroscopy was used to study the optical properties of ZnO and Ni-ZnO materials. Optical absorption spectra of ZnO and Ni-ZnO were studied in the wavelength range 375–800 nm shown in Fig. 2a. The band gap of ZnO and Ni-ZnO materials were calculated by using Eq. (1) [43].

$$(\alpha h\nu) = (Eg - h\nu)^n \quad (1)$$

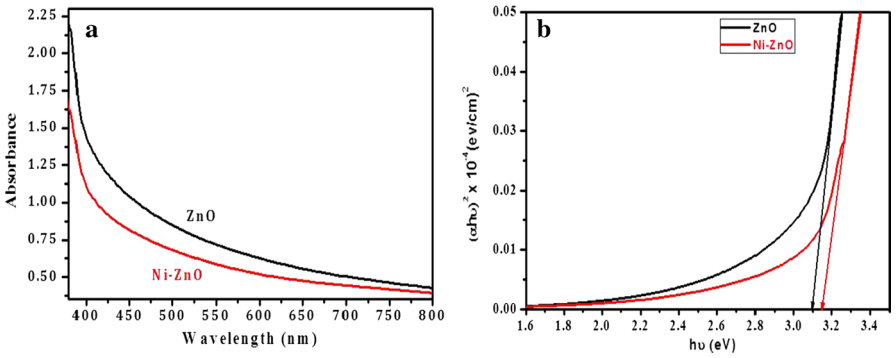

Fig. 2 **a** Optical absorption spectrum and **b** $(\alpha h\nu)^2$ versus hν plot of Ni-ZnO and ZnO

where '$h\nu$' is the incident photon energy, 'α' is an absorption coefficient, 'A' is a constant and 'n' determines electronic transition. The band gap of ZnO and Ni-ZnO were determined by plotting the graph of $(\alpha h\nu)^2$ versus $h\nu$ in Fig. 2b. The linear portion of the plot is extrapolated to the X-axis to measure the exact band gap. The band gap is 3.09 eV for ZnO nanoflakes and 3.18 eV for Ni-ZnO nanoparticles. The band gap for Ni-ZnO nanoparticles (3.18 eV) is increased than ZnO nanoflakes (3.09 eV) showing lower particle size. This increase in band gap for Ni-ZnO nanoparticles confirms the incorporation of Ni^{++} on the Zn^{++} site of the ZnO lattice, which proves the doping of Ni in ZnO. We have obtained different band gaps for ZnO nanoflakes and Ni-ZnO nanoparticles compared with earlier reported results [44].

Structural study of ZnO and Ni-ZnO

The structural properties of ZnO and Ni-ZnO were studied by using the XRD technique. The XRD patterns of the ZnO and Ni-ZnO nanoparticles are shown in Fig. 3. The XRD patterns of the ZnO nanoflakes show a polycrystalline nature. The XRD patterns of the ZnO and Ni materials are in agreement with JCPDS card nos. 05-0664 and 75-0197, respectively. The XRD patterns of the ZnO material show a maximum intensive *hkl* plane (101) at 2θ 36.34°. The asterisk (*) indicates the peak of nickel with a *hkl* plane (200) at 2θ 43.30°, which proves the doping of Ni in ZnO. The lattice spacing d was calculated by using Bragg's diffraction law in Eq. (2)

$$2d \sin\theta = n\lambda \tag{2}$$

where 'λ' is the wavelength of the X-rays, 'n' is the order of diffraction and 'θ' is a diffraction angle. Table 1 shows the 2θ, respective *hkl* planes, observed d values and standard d values of Ni-ZnO nanoparticles.

The crystallite sizes (D) of ZnO and Ni-ZnO were calculated by the Debye–Scherrer formula, shown in Eq. (3) [45].

$$D = \frac{k\lambda}{\beta \cos\theta} \tag{3}$$

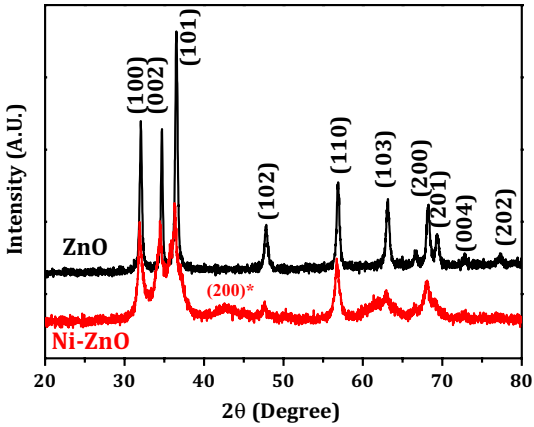

Fig. 3 XRD patterns for ZnO nanoflakes and Ni-ZnO nanoparticles

Table 1 The 2θ, *hkl* planes, observed and standard '*d*' values of Ni-ZnO nanoparticles

Sr. no.	2θ (°)	*hkl* planes	Observed '*d*' values	Standard '*d*' values
1	31.72	100	2.8180	2.8160
2	34.50	002	2.6045	2.6020
3	36.34	101	2.4700	2.4760
4	43.30	200 (Ni)*	2.0872	2.0850
5	47.75	102	1.9100	1.9110
6	56.60	110	1.6240	1.6260
7	62.95	103	1.4766	1.4770
8	66.45	200	1.4070	1.4070
9	69.10	201	1.3585	1.3590
10	72.70	004	1.3010	1.3010
11	77.05	202	1.2376	1.2380

* Doping of Nickel

where 'λ' is a wavelength of the X-rays, 'θ' is the Bragg's angle, 'K' is a constant and 'β' is the full width at half maximum. The crystallite size of the more intensive peak (101) of ZnO material is 24.28 nm; however, for Ni-ZnO it is found to be 12.15 nm. The results show a decrease in crystallite size when nickel is doped in ZnO material.

Surface morphology of ZnO nanoflakes and Ni-ZnO nanoparticles

The surface morphology of the materials was analyzed by using the SEM technique. Higher and lower magnification images of ZnO nanoflakes are shown in Fig. 4a and b, respectively, and of Ni-ZnO nanoparticles in Fig. 4c and d, respectively. The surface morphology of the ZnO material shows nanoflakes; however, the Ni-ZnO material displays a granular nanoparticulate like morphology. The ZnO nanoflakes show 40 nm width and about 60 nm length, while the Ni-ZnO nanoparticles show

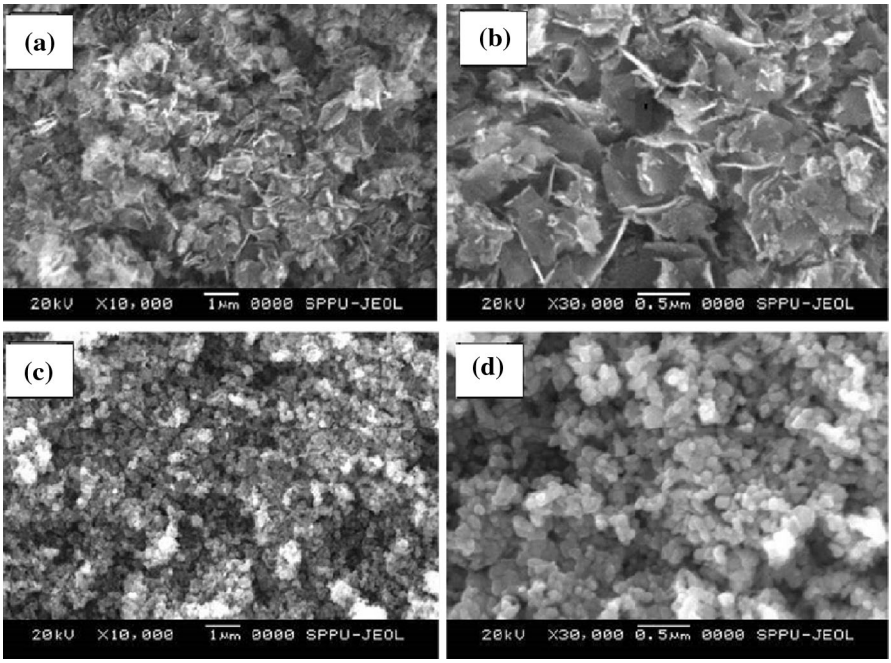

Fig. 4 SEM images (**a** and **b**) for ZnO nanoflakes and (**c** and **d**) for Ni-ZnO nanoparticles at lower and higher magnifications, respectively

an average grain size of 80 nm. It is observed that, when Ni is doped in ZnO, the surface morphology of ZnO is changed from nanoflakes to nanoparticles due to the doping of nickel, which proves that nickel was doped successfully in the Ni-ZnO nanoparticles. This result is in accordance with the UV and XRD analyses.

Composition study of ZnO nanoflakes and Ni-ZnO nanoparticles

The chemical compositions of ZnO and Ni-ZnO nanoparticles were analyzed by the EDAX technique, as shown in Fig. 5. The presence of peaks at 0.270 and 1.260 keV for ZnO in Fig. 5a confirms the presence of O and Zn, respectively. The presence of peaks at 0.525, 0.851 and 1.012 keV for Ni-ZnO in Fig. 5b confirms the presence of O, Ni and Zn, respectively. The peak at 0.851 keV confirms the doping of Ni in ZnO. This result is in accordance with the UV, XRD, and SEM analyses of the ZnO nanoflakes and Ni-ZnO nanoparticles.

Effect of amount of catalyst on synthesis of DHPMs

The reaction of aldehyde (1 mmol), ethyl acetoacetate (1 mmol) and urea (1 mmol) in the presence of catalytic amounts of Ni-ZnO nanoparticles and ZnO nanoflakes in the hydrotropic aqueous solution of NaPTS at room temperature with stirring condition resulted into 3,4-dihydropyrimidin-2(1H)-ones (Scheme 1).

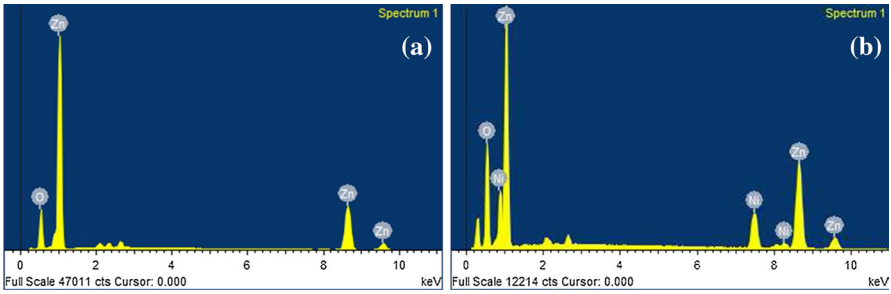

Fig. 5 EDAX patterns for (**a**) ZnO and (**b**) Ni-ZnO nanoparticles

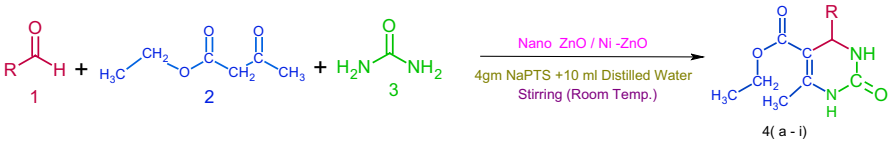

Scheme 1 The Biginelli reaction between aromatic aldehyde, ethyl acetoacetate and urea. *Reaction condition*: Aldehyde (1 mmol), ethyl acetoacetate (1 mmol), Urea (1 mmol), [a]nanocatalyst (mol%), [b]NaPTS, [c]yield (%) and distilled water (10 mL)

Lower yields were obtained with lower amounts of the catalysts used, e.g., 8 mol% (Fig. 6). The yield was not increased to much extent when there was a further rise in the amount of catalyst, e.g., more than 8 mol%. Ni-ZnO nanoparticles (8 mol%) and ZnO nanoflakes (8 mol%) show an excellent yield of product. We achieved 96% yield of DHPMs at 8 mol% of nanocatalysts. Ni-ZnO nanoparticles showed better results than ZnO nanoflakes (Fig. 6). It was observed that, due to a decrease in particle size for Ni-ZnO nanoparticles, the catalytic activity of Ni-ZnO is much increased compared with ZnO nanoflakes in water. The proposed reaction was completed in the absence of a nanocatalyst with 80% yield in the longer reaction time of 7 h. The time of the reaction was decreased up to 1.8 h in the presence of the Ni-ZnO nanocatalyst (Fig. 7). The yield of the product was increased to 96% for 8 mol% of the Ni-ZnO nanocatalyst (Fig. 6).

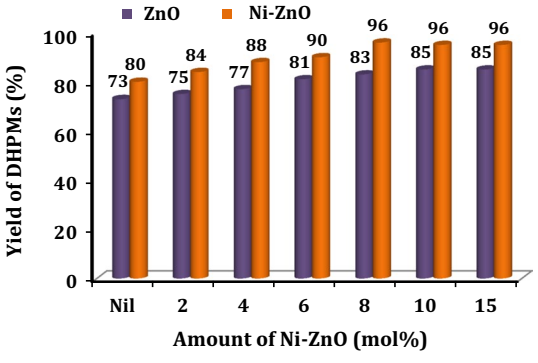

Fig. 6 Effect of the amount of Ni-ZnO nanocatalyst on the yield for DHPMs

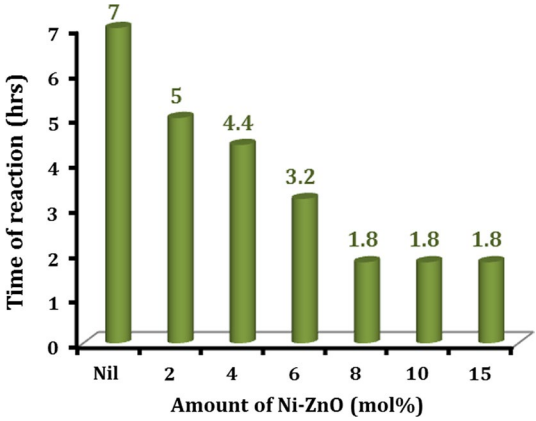

Fig. 7 Effect of the amount of Ni-ZnO nanoctalyst on the time of the reaction

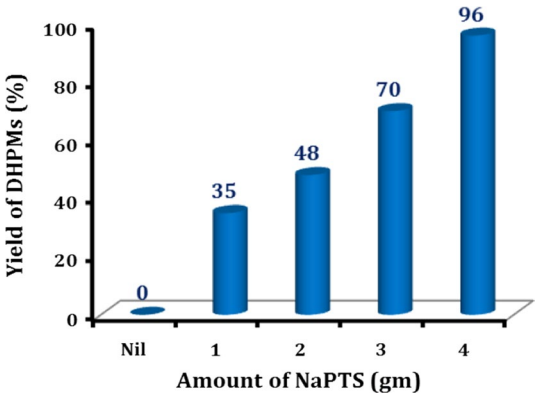

Fig. 8 Effect of NaPTS on the yield of DHPMs

Effect of NaPTS on synthesis of DHPMs

A one-pot synthesis of DHPMs is not possible without a solvent with the stirring condition at room temperature. We used distilled water as a solvent for DHPMs syntheses and also used NaPTS for completely dissolving the reactants in water. DHPMs were without a yield only in the presence of water as the solvent at room temperature due to the dissolving problem of organic reactants in water; hence, NaPTS was used to make the organic reactants soluble in water (Fig. 8). DHPMs were synthesized with 35 and 96% yields for 1 and 4 g of NaPTS, respectively. The yield of the product was increased with increasing amounts of NaPTS. We obtained a 96% yield of DHPM for 4 g of NaPTS. Various aromatic aldehydes, ethyl acetoacetate and urea showed excellent solubility in water for 4 g of NaPTS (Fig. 8).

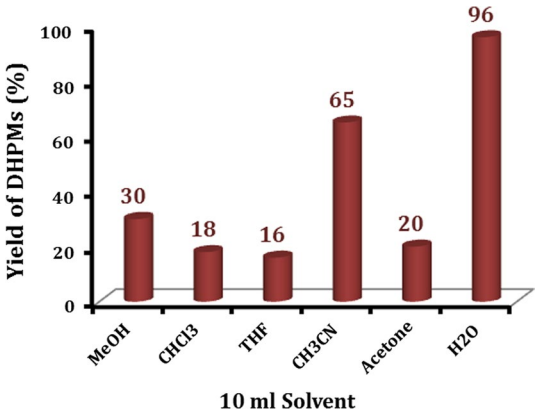

Fig. 9 Effect of solvent on the yield of DHPMs

Effect of solvent on the synthesis of DHPMs

We successfully synthesized DHPMs with outstanding yields in water as a solvent because NaPTS shows good activity in the presence of water. Here, in the case of the proposed reaction, NaPTS completely dissolves the reactants only in water and not in the tested organic solvents like methanol, chloroform, acetone, or acetonitrile. We successfully synthesized DHPMs in the presence of ZnO nanoflakes and Ni-ZnO nanoparticles. In our study, It was observed that water is the best solvent in terms of yield compared with methanol, chloroform, acetone, and acetonitrile (Fig. 9). To the best of our knowledge, the Ni-ZnO nanocatalyst shows excellent catalytic activity in water and is very stable, as shown in (Fig. 9). This is a much greener approach than any other existing methodologies for the synthesis of DHPMs.

Recyclability of Ni-ZnO nanoparticles and ZnO nanoflakes

Successive condensations of benzaldehyde, ethyl acetoacetate and urea were carried out to check the reusability of the Ni-ZnO nanoparticles and ZnO nanocatalyst. Yields were between 94 and 96% with the reusability of nanocatalysts (Fig. 10). The nanocatalyst was centrifuged at 4000 rpm from the final product during work-up and settled at the bottom. It was then dried at 120 °C in a hot-air oven and reused five times in reactions. It was observed that the nanocatalyst showed the same activity during its recycling process for the proposed reaction.

The rate of reaction is affected by the size of nanoparticles. Nanocatalysts with smaller particle sizes give a more effective yield than nanocatalysts with larger particle sizes. Ni-ZnO nanoparticles have an average particle size of 80 nm whereas ZnO nanoflakes are 40 nm in width and about 60 nm in length. The results show that Ni-ZnO nanoparticles are smaller in particle size and higher in surface area (due to the smaller particle size) than ZnO nanoflakes. Therefore, the yield of DHPMs is much better in the presence of Ni-ZnO nanoparticles than ZnO nanoflakes (Table 2).

The yield of DHPMs is excellent and increased from 15–40% to 92–96% in water as a solvent. Aromatic rings containing electron-withdrawing groups such

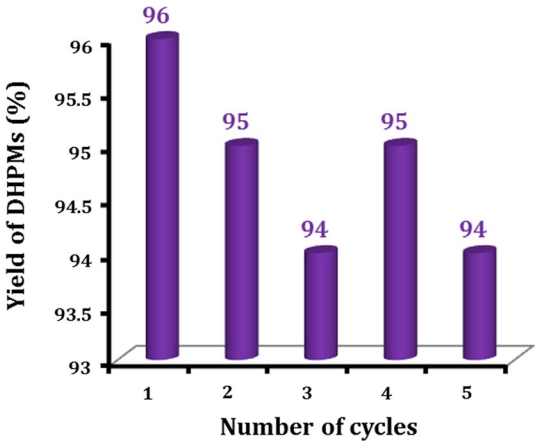

Fig. 10 Recyclability for Ni-ZnO nanoparticles

Table 2 Effect of Ni-ZnO nanoparticles and ZnO nanoflakes on the time of reaction and the yield in [b]NaPTS

DHPMs	Substrate (R)	[a]Nanocatalyst	Time (h)	[c]Yield (%)
4a	C_6H_5	Ni-ZnO	1.8	92
		ZnO	3.0	85
4b	2-(OH)-4-(OMe)-C_6H_3	Ni-ZnO	2.0	90
		ZnO	3.5	86
4c	4-Br-C_6H_4	Ni-ZnO	1.5	94
		ZnO	2.5	86
4d	4-(NO_2)-C_6H_4	Ni-ZnO	1.5	94
		ZnO	2.5	84
4e	4-Cl-C_6H_4	Ni-ZnO	1.4	96
		ZnO	2.5	87
4f	3,4-(OMe)-C_6H_3	Ni-ZnO	1.9	94
		ZnO	3.0	90
4g	4-(OMe)-C_6H_4	Ni-ZnO	1.5	92
		ZnO	2.5	90
4h	3-(Br)-C_6H_4	Ni-ZnO	1.4	94
		ZnO	2.4	84
4i	4-(CH_3)-C_6H_4	Ni-ZnO	1.7	94
		ZnO	2.6	92
4j	3,4,5-(OMe)-C_6H_3	Ni-ZnO	1.6	96
		ZnO	2.5	90

Reaction condition: Aldehyde (1 mmol), ethyl acetoacetate (1 mmol), Urea (1 mmol), [a]nanocatalyst (8 mol%), [b]NaPTS (4 g), [c]yield (%) and distilled water (10 mL)

as bromine, chlorine, and the nitro group were easily converted into the respective 3,4-dihydropyrimidinones and gave excellent yields (Table 2, entries **4c**, **4e**, **4d**, **4h**). The rate of reaction and yield is increased because the carbonyl carbon of aromatic

aldehyde becomes electron-deficient due to the electron-withdrawing group which leads to an effective nucleophilic attack. Aromatic rings containing electron-donating groups like (OCH_3), OH, CH_3 groups also give yields of more than 90%, even though there is an electron-donating effect (Table 2, entries **4f**, **4g**, **4i**, **4j**). This is seen because NaPTS completely the dissolves reactants in water.

The structures and melting points of the DHPMs are as shown in Table 3.

Spectroscopic data of some synthesized dihydropyrimidones

***4c**: Ethyl4-(4-bromophenyl)-6-methyl-2-oxo-1,2,3,4-tetrahydropyrim idine-5-carboxylate*

(Table 3, Entry 4c) IR ν_{max} (KBr) 3385(NH), 1724(–O–CO–), 1649(–CO–N), 1460(C=C), 610(C–Br) cm^{-1} **^{1}H-NMR ($CDCl_3$, 400 MHz)** δ:1.21(t,3H), 2.27(s,3H), 4.01 (q,2H), 5.27 (s,1H), 6.58 (s,2H), 7.15(d,2H), 7.36(d,2H,) **^{13}C-NMR ($CDCl_3$,100 MHz)** δ: 14.43 (CH_2–$\underline{CH_3}$), 15.03(CH_3), 49.15 (C-4), 61.08 ($\underline{CH_2}$–CH_3), 106.03 (C-5), 121.18 (C-4′), 129.35 (C-2′, C-6′), 131.33 (C-3′, C-5′), 142.25 (C-1′), 148.21 (C-6), 150.10 (–$\underline{C}$=O), 165.40 (Et-O-$\underline{C}$=O). The spectroscopic values are shown in supplementary data (SD1).

***4e**: Ethyl4-(4-chlorophenyl)-6-methyl-2-oxo-1,2,3,4-tetrahydropyrimidine-5-carboxylate*

(Table 3, Entry 4e) IR ν_{max} (KBr) 3416(NH), 1728(–O–CO–), 1664(–CO–N), 1462(C=C), 700(C–Cl) cm^{-1} **^{1}H-NMR ($CDCl_3$, 400 MHz)** 1.10 (t, 3H), 2.17 (s, 3H), 3.93 (q,2H), 5.20 (d,1H, H-4), 6.07(s,2H), 7.04 (d, 2H, H-2′, H-6′), 7.18 (d,2H, H-3′, H-5′), **^{13}C-NMR ($CDCl_3$,100 MHz)** δ:14.51 (CH_2–$\underline{CH_3}$), 15.31(CH_3), 50.12 (C-4), 61.30 ($\underline{CH_2}$–CH_3), 106.53(C-5), 128.50 (C-2′, C-6′), 130.81 (C-3′, C-5′), 133.11 (C-1′), 143.51 (C-4′), 147(C-2), 153.21(C-6), 170.01(Et-O$\underline{C}$=O) The spectroscopic values are shown in supplementary data (SD2).

***4g**: Ethyl4-(4-methoxyphenyl)-6-methyl-2-oxo-1,2,3,4-tetrahydropyrimidine-5-carboxylate*

(Table 3, Entry-4g) IR ν_{max} (KBr) 3442(NH), 1734(–O–CO–), 1647(–CO–N), 1445(C=C), 1219(C–O–C) cm^{-1} **^{1}H-NMR ($CDCl_3$ 400 MHz)** δ: 1.20(t, 3H), 2.34(s,3H), 3.91(s,3H), 4.09(q, 2H), 5.35 (s,1H), 5.96 (s,2H), 6.84(d,2H H-3′ & H-5′), 7.28(d, 2H, H-2′ & H-6′) **^{13}C-NMR ($CDCl_3$, 100 MHz)** δ: 14.27 (CH_2–$\underline{CH_3}$), 16.79(CH_3), 49.69 (C-4), 55.79 (–O–CH_3), 61.07 ($\underline{CH_2}$–CH_3), 106.76 (C-5), 114.64 (C-2′, C-6′), 127.20 (C-3′, C-5′), 135.42 (C-1′), 145.62 (C-6), 150.25 (–$\underline{C}$=O), 158.21 (C-4′), 167.09 (Et-O-$\underline{C}$=O). The spectroscopic values are shown in supplementary data (SD3).

Table 3 Biginelli reactions of various aromatic aldehydes, ethyl acetoacetate and urea

DHPMs	Aromatic Aldehydes	Ethyl Aceto Acetate	Urea	Product	M.P (^{0}C) Found
4a	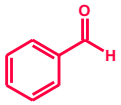	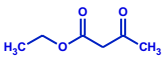	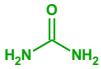	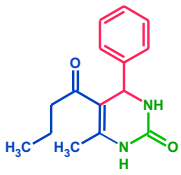	203
4b	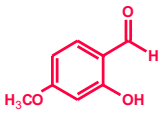	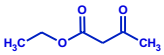	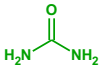	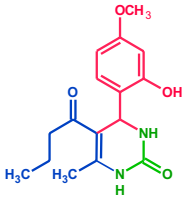	234
4c	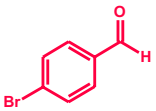	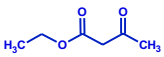	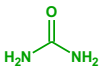	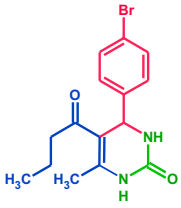	214
4d	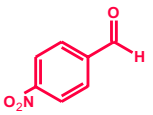	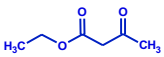	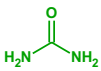	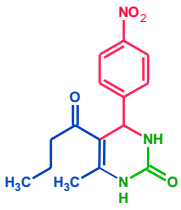	207
4e	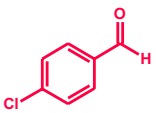	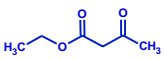	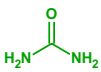	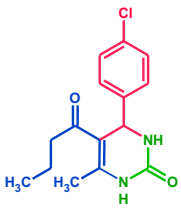	214
4f	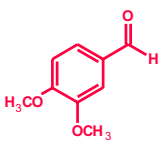	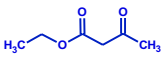	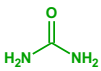	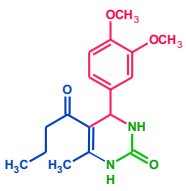	176

Table 3 (continued)

DHPMs	Aromatic Aldehydes	Ethyl Aceto Acetate	Urea	Product	M.P (^{0}C) Found
4g	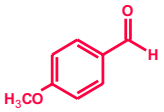	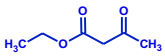	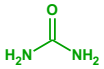	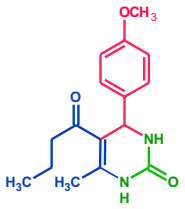	202
4h		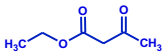	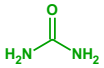	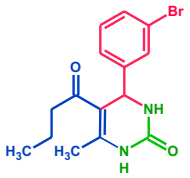	185
4i	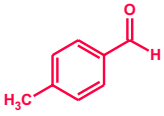	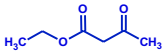	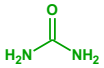	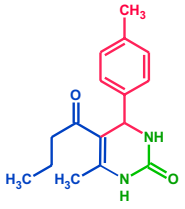	212
4j	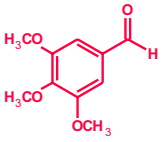	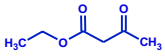	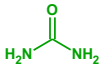	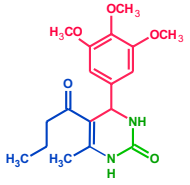	160

***4h**: Ethyl 4-(3-bromophenyl)-6-methyl-2-oxo-1,2,3,4-tetrahydropyrimidine-5-carboxylate*

(Table 3, Entry 4h) IR ν_{max} (KBr) 3350(NH), 1730(–O–CO–), 1633(–CO–N), 1450(C=C), 685(C–Br) cm^{-1} **^{1}H-NMR ($CDCl_3$ 400 MHz)** δ: 1.21(t, 3H), 1.89(s,3H), 4.07 (q, 2H), 5.36 (s,1H), 6.07 (s,2H), 7.28(m,4H H-2′, H-4′ H-5′, H-6′), **^{13}C-NMR ($CDCl_3$, 100 MHz)** δ: 14.15 (CH_2–$\underline{CH_3}$), 15.00(CH_3), 55.30 (C-5), 60.20 ($\underline{CH_2}$–CH_3), 106.82(C-1) 122.64 (C-3′), 125.37 (C-6′), 130.37 (C-4′), 131.08 (C-5′), 132.31(C-2′), 145.85(C-1′), 146.71(C-2), 150.19(C-4),165.34 (Et-O-$\underline{C}$=O). The spectroscopic values are shown in supplementary data (SD4).

***4j**: Ethyl 6-methyl-2-oxo-4-(3,4,5-trimethoxyphenyl)-1,2,3,4-tetrahydro-pyrimidine-5-carboxylate*

(Table 3, Entry 4j) IR ν_{max} (KBr) 3433(NH), 1749 (–O–CO–), 1684(–CO–N), 1592(C=C), 1232(C–O–C) cm^{-1} **^{1}H-NMR ($CDCl_3$, 400 MHz)** δ: 1.33(t, 3H), 1.77(s,3H), 3.83(s,3H), 3.84(s,3H), 3.95(s,3H), 4.02 (q, 2H), 5.65 (s,1H), 6.07 (s,2H), 6.15(s,2H H-2′ & H-6′), **^{13}C-NMR ($CDCl_3$, 100 MHz)** δ: 15.67 (CH_2–$\underline{CH_3}$), 17.79(CH_3), 50.29 (C-5), 56.29 (–O–$\underline{C}H_3$), 61.01 ($\underline{CH_2}$–CH_3), 104.38 (C-2′, C-6′), 106.47(C-1) 137.72 (C-1′, C-4′), 147.62 (C-2), 150.25 (–$\underline{C}$=O), 150.66 (C-3′, C-5′), 165.74 (Et-O-$\underline{C}$=O). The spectroscopic values are shown in supplementary data (SD5).

The above described products have been confirmed by IR, ^{1}H-NMR and ^{13}C-NMR.

Conclusion

We successfully synthesized Ni-ZnO nanoparticles and ZnO nanoflakes by the co-precipitation method and characterized them by various analytical techniques. An increase in band gap is found when Ni is doped insitu ZnO. The crystallite size is found to be 24.28 and 12.15 nm for ZnO nanoflakes and Ni-ZnO nanoparticles, respectively. The decrease in crystallite size and the change in surface morphology from nanoflakes to nanoparticles is observed due to doping of Ni in ZnO. We carried out the synthesis of DHPMs in organic solvent-free condition, i.e. in distilled water, successfully for the first time under room temperature condition using ZnO nanoflakes and Ni-ZnO nanoparticles. Ni-ZnO shows excellent yields of DHPMs because the particle size of Ni-ZnO is smaller and, hence, this results in a larger surface area for the proposed reaction compared with the ZnO nanoflakes. Therefore, the Ni-ZnO nanocatalyst is a much better aqueous hydrotropic nanocatalyst for the synthesis of biologically active DHPMs at room temperature than the ZnO nanoflakes.

Acknowledgement Authors are grateful to the Department of Chemistry, Yashavantrao Chavan Institute of Science, Satara, for providing the laboratory facility to complete this work.

References

1. B. Hu, J. Pan, H.L. Yu, J.W. Liu, J.H. Xu, Process. Biochem. **44**, 1019 (2009)
2. S. Asghari, M. Mohammdania, Res. Chem. Intermed. **43**, 6701 (2017)
3. M. Gopiraman, S. Sarvanamoorthy, M. Chung, Res. Chem. Intermed. **43**, 5601 (2017)
4. S. Ganesh Babu, R. Karvembu, Catal. Surv. Asia **17**, 156 (2013)
5. P. Biginelli, Gazzetta Chimica Italiana **23**, 360 (1893)
6. S. Majumdar, J. De Pal, I. Ghosh, R.K. Nath, S. Chowdhury, D. Roy, D.K. Maiti, RSC Adv. **5**, 24681 (2015)
7. K.S. Atwal, B.N. Swanson, S.E. Unger, D.M. Floyd, S. Moreland, A. Hedberg, B.C. O'Reill, J. Med. Chem. **34**, 806 (1991)
8. C.O. Kappe, W.M.F. Fabian, Tetrahedron **53**, 2803 (1997)

9. K.S. Atwal, G.C. Roonyak, B.C. O'Reilly, J. Schwartz, J. Org. Chem. **54**, 5898–5907 (1989)
10. A.D. Patil, N.V. Kumar, W.C. Kokke, M.F. Bean, A.J. Freyer, C.D. Brosse, S. Mai, A. Truneh, D.J. Faulkner, J. Org. Chem. **60**, 1182 (1995)
11. B.B. Snider, V. Chen, A.D. Patil, A. Freyer, Tetrahedron Lett. **37**, 6977 (1996)
12. C.O. Kappe, Tetrahedron **49**, 6937 (1993)
13. B.C. Ranu, A. Hazra, U.J. Jana, J. Org. Chem. **65**, 6270 (2000)
14. J.S. Yadav, B.V.S. Reddy, J.J. Naidu, K. Sadashiv, Chem. Lett. **33**, 926 (2004)
15. B. Gangadasu, S. Palaniappan, V.J. Rao, Synlett **7**, 1285 (2004)
16. M. Nasr-Esfahani, M. Taei, RSC Adv. **5**, 44978 (2015)
17. A.V. Narsaiah, B.K. Nagaiah, Synthesis **8**, 1253 (2004)
18. H. Hazarkhani, B. Karimi, Synthesis **8**, 1239 (2004)
19. K.A. Kumar, M. Kasthuraiah, C.S. Reddy, D. Reddy, Tetrahedron Lett. **42**, 7873 (2001)
20. C.V. Reddy, M. Mahesh, P.V.K. Raju, R. Babu, V.V.N. Reddy, Tetrahedron Lett. **43**, 2657 (2002)
21. S.L. Jain, J.K. Joseph, B. Sain, Catal. Lett. **115**, 52 (2007)
22. A. Zhu, Q. Li, L. Li, J. Wang, Catal. Lett. **143**, 463 (2013)
23. R. Varala, M.M. Alam, S.R. Adapa, Synlett **1**, 67 (2003)
24. A.K. Mitra, K. Banerjee, Synlett **10**, 1509 (2003)
25. V.R. Rani, N. Srinivas, M.R. Kishan, S.J. Kulkarni, K.V. Raghavan, Green Chem. **3**, 305 (2001)
26. T. Raja, B. Kaur, N. Kaur, N. Singh, RSC Adv. **5**, 46654 (2015)
27. S.K. De, R.A. Gibbs, Synthesis **11**, 1748 (2005)
28. I. Cepanec, M. Litvic, A. Bartolincic, M. Lovric, Tetrahedron **61**, 4275 (2005)
29. G.L. Zhang, H.X. Cai, Synth. Comm. **35**, 829 (2005)
30. I. Saxena, D.C. Borah, J.C. Sarma, Tetrahedron Lett. **46**, 1159 (2005)
31. Y.L. Zhu, Y.J. Pan, S.L. Huang, Synth Comm. **34**, 3167 (2004)
32. M.M. Heravi, K. Bakhtiari, F.F. Bamoharram, Catal. Commun. **7**, 373 (2006)
33. Y. Qian, C. Ma, L. Wang, M. Yang, J. Org. Chem. **65**, 3864 (2000)
34. J. Lu, H. Ma, Synlett **1**, 63 (2000)
35. H.A. Stefani, P.M. Gatti, Synth. Commun. **30**, 2165 (2000)
36. A.R. Gholap, K. Venkatesan, T. Daniel, R.J. Lahoti, K.V. Srinivasan, Green Chem. **6**, 147 (2004)
37. S.L. Jain, S. Singhal, B. Sain, Green Chem. **9**, 740 (2007)
38. A. Lavergne, L. Moity, V. Molinier, J.M. Aubry, RSC Adv. **3**, 5997 (2013)
39. S. Subramaniam, A. Palanisamya, A. Sivasubramanian, RSC Adv. **5**, 7479 (2015)
40. J. Eastoe, M.H. Hatzopoulos, P.J. Dowding, Soft Mater. **7**, 5917 (2011)
41. R. Sedghi, M. Shariati, M.R. Zarehbin, A.A. Soorki, J. Alloys Compd. **729**, 921–928 (2017)
42. P. Bai, P. Wu, Z. Yan, J. Zhou, X.S. Zhao, J. Phys. Chem. C **111**, 9729 (2007)
43. P.K. Pagare, A.P. Torane, Microchim. Acta. **183**, 2983 (2016)
44. R. Sedghi, M.R. Mabid, M. Shariati, M. Behbahani, H.R. Moazzami, Fibers Polym. **17**, 1969 (2016)
45. P. Bai, B. Liu, P. Wu, R. Ullah, W. Xing, Z. Yan, Sci. China Mater. **60**, 985 (2017)